REPORT DOCUMENTATION PAGE

Form Approved
OMB No. 0704-0188

1. REPORT DATE *(DD-MM-YYYY)*

2. REPORT TYPE
Final

3. DATES COVERED *(From - To)*
10/1/01-9/30/05

4. TITLE AND SUBTITLE
Fundamental Studies of Inkjet Based Fuel Injection Technology For Pulsed Detonation Engines

5a. CONTRACT NUMBER

5b. GRANT NUMBER
F49620-02-1-0133

5c. PROGRAM ELEMENT NUMBER

6. AUTHOR(S)
John W. Daily

5d. PROJECT NUMBER

5e. TASK NUMBER

5f. WORK UNIT NUMBER

7. PERFORMING ORGANIZATION NAME(S) AND ADDRESS(ES)

University of Colorado at Boulder
Mechanical Engineering Department
Boulder, CO 80309-0427

8. PERFORMING ORGANIZATION REPORT NUMBER

9. SPONSORING / MONITORING AGENCY NAME(S) AND ADDRESS(ES)
AFOSR

10. SPONSOR/MONITOR'S ACRONYM(S)

11. SPONSOR/MONITOR'S REPORT NUMBER(S)

12. DISTRIBUTION / AVAILABILITY STATEMENT

Approved for public release,
distribution unlimited

AFRL-SR-AR-TR-07-0386

13. SUPPLEMENTARY NOTES

14. ABSTRACT

The University of Colorado, in collaboration with TDA Research Inc., worked on using inkjet type concepts to develop MEMS technology for fuel injection for pulsed detonation engines (PDE). We considered this approach because of the requirements of periodic injection, small droplet size and distributed injection. We demonstrated the potential for injectors based on inkjet technology to meet PDE needs. We evaluated commercially available inkjet technologies, developed a large array atomizer conceptual design, and reviewed and compared current atomization techniques to military specifications. The results of our study showed that new injection technology would be required and that inkjet-type MEMS technology does have the potential to meet PDE needs. During the first year of the AFOSR program we explored issues such as material compatibility, flow throughput, and actuation design. We carried out finite element stress analysis simulations for various pump configurations and volume of fluid (VOF) analysis of jet breakup. During the second year our work focused on developing comprehensive simulations of real pump designs. We successfully modeled a passive valve pump and showed that the simulation correctly predicts behavior observed in the literature. During the final year of funding we focused on design optimization using multi-physics simulations and assisting in prototype testing.

15. SUBJECT TERMS

16. SECURITY CLASSIFICATION OF:			**17. LIMITATION OF ABSTRACT**	**18. NUMBER OF PAGES**	**19a. NAME OF RESPONSIBLE PERSON**
a. REPORT	**b. ABSTRACT**	**c. THIS PAGE**			**19b. TELEPHONE NUMBER** *(include area code)*

Standard Form 298 (Rev. 8-98)
Prescribed by ANSI Std. Z39.18

20071015195

I. Introduction

This final report details accomplishments on AFOSR grant #F49620-02-1-0133 titled "Fundamental Studies of Inkjet Based Fuel Injection Technology for Pulsed Detonation Engines."

During the grant period, we worked on using inkjet type concepts to develop MEMS technology for fuel injection for pulsed detonation engines (PDE). We considered this approach because of the requirements of periodic injection, small droplet size and distributed injection. As part of a Phase I SBIR effort sponsored by the Office of Naval Research, TDA Research, Inc. and the University of Colorado at Boulder demonstrated the potential for injectors based on inkjet technology to meet PDE needs. We evaluated commercially available inkjet technologies, developed a large array atomizer conceptual design, and reviewed and compared current atomization techniques to military specifications. The results of our study showed that new injection technology will be required and that inkjet-type MEMS technology does have the potential to meet PDE needs.

Subsequently, TDA Research applied for, and was awarded, Phase II support with ONR to carry out applied development of an inkjet technology based fuel injector for the PDE. The University of Colorado served as a sub-contractor, providing design and fabrication support utilizing laboratory facilities at the University. In parallel, and under AFOSR support, the University of Colorado provided basic research support for the project. During the first year of the AFOSR program we explored issues such as material compatibility, flow throughput, and actuation design. We carried out finite element stress analysis simulations for various pump configurations and volume of fluid (VOF) analysis of jet breakup. During the second year our work focused on developing comprehensive simulations of real pump designs. We successfully modeled a passive valve pump and showed that the simulation correctly predicts behavior observed in the literature. During the final year of funding we focused on design optimization using multi-physics simulations and assisting in prototype testing.

II. Progress

During the first year, effort was devoted to establishing that MEMS based technologies would be suitable for the PDE application. We explored issues such as material compatibility, flow throughput, and actuation design. We carried out finite element stress analysis simulations for various pump configurations and VOF analysis of jet breakup. During the second year our work focused on developing comprehensive simulations of real pump designs. We successfully modeled a passive valve pump and showed that the simulation correctly predicts behavior observed in the literature. During the final year we continued modeling work in support of device development and prototype testing. We describe these accomplishments in more detail below.

On July 18, 2003 a provisional patent application was filed with the United States Patent and Trademark Office titled "Micro Conformal-Array Liquid Atomizer." The disclosure

was for work performed under ONR contract. It was our intention to convert the application to a standard application prior to July 18, 2004. However, upon advice of patent attorneys we decided instead to apply for patents on specific devices.

Because of intellectual property considerations we have been extremely cautious about publishing our work. We have presented five conference papers [1-5] and a paper on analytic modeling of the pump system will appear in the AIAA Journal of Propulsion and Power [6]. However, during the project we have kept our project monitors fully informed [7-9]. As mentioned above, our AFOSR work was carried out in collaboration with TDA Research, Inc. TDA was funded via an SBIR by ONR. Our ONR contract monitor was Dr. Chris Brophy of the Naval Postgraduate School in Monterey, California. Dr. Brophy is conducting tests of various air-breathing pulsed detonation engine concepts. In addition to giving Dr. Brophy regular briefings on the ONR supported work, we kept him informed of the AFOSR supported work. We have also consulted with him on PDE issues as they relate to fuel injection.

The potential of MEMS atomizers has attracted considerable outside interest from advanced engine and specialty product developers. In order to pursue those business opportunities we established several Confidentiality Disclosure Agreements (CDAs) with industry leading companies. We received a Phase I SBIR contract from the Air Force to apply the MEMS atomizer technology to gas turbines. Also, of particular interest to the US Armed Forces are miniature (100 to 1000 W) engine/generator units under development by Aerodyne Research, Inc. (ARI) for portable electric power generation using JP-8, diesel, and kerosene-type fuels. High fuel efficiency in small-scale engines requires droplets smaller than 20 microns to be produced using very little parasitic power for atomization. Aerodyne plans to subcontract us to provide a MEMS atomizer design and prototype under an Army Phase II SBIR. Advanced Ceramics Research needs improved atomization and fuel flow control to meet desired Silver Fox UAV endurance goals, despite already holding the world's endurance record in its size class (20 hours on less than a gallon of JP-8). TDA also just signed a CDA with AAI Corporation for UAV small engines. They have developed tactical UAVs, such as Pioneer and Shadow for the Army, and are in similar need of improved combustion. Peak Materials approached TDA seeking fine droplet atomization for nanomaterial vapor deposition equipment. They greatly desire atomized sprays containing small monodisperse droplets to form very uniform coatings. Unfortunately, current atomization technologies produce relatively low quality coatings due to their large droplet distribution, whereas inkjets have already demonstrated the ability of MEMS atomizers to produce nearly monodisperse droplets.

Most recently we obtained SBIR funding from the National Science Foundation (Start July 1, 2007) to continue work on the MEMS atomizer concept with application to small carbureted engines.

a. Droplet Formation

Our initial design ideas mainly focused on the generation of small diameter jets. The properties of the fluid and nozzle geometry will determine the mechanism by which a liquid jet will collapse and breakup into droplets. Rayleigh breakup of a laminar jet is expected for flow conditions through small nozzles (refer to Figure 1 for Re < 10 and Z ~ 0.25). Fluid is expelled from a nozzle as a small diameter jet, which breaks up due to the growth of surface tension induced instabilities as illustrated in Figure 1. The small droplets formed are approximately proportional to twice the nozzle diameter, but smaller satellite droplets can also occur. These droplets will be stable and not undergo additional breakup. Therefore, for steady state round jet injection designs, channels diameters must be on the order of a few microns to meet our design objectives. The minimum droplet size from Rayleigh breakup is about 4 μm at the minimum feature size using MUMPs, SUMMIT, or laser drilling processes.

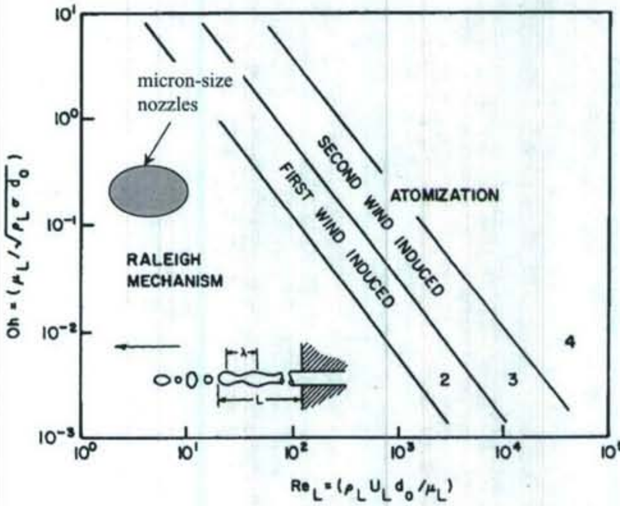

Figure 1. Jet breakup mechanisms. [4]

It has been shown that forcing droplet breakup at the jet natural frequency results in smaller and nearly monodisperse droplets. The Rayleigh droplet breakup of a jet may be forced at its natural frequency by coupling the actuation to the characteristics of the fluid and the nozzle geometry. This frequency from Weber's theory of disintegration is given by:

$$f = \frac{u_{jet}}{\sqrt{2}\pi d_n (1+3Z)^{1/2}}$$

where $d_{droplet} = 1.89 * d_n$, and Ohnesorge number $Z = \frac{\mu}{\sqrt{\rho \sigma d_n}}$. The advent of MEMS technology might make forcing practical at the micro-scale.

However, jet injection does not appear to be the optimum means to obtain both small droplets and reasonable flow rates. As shown in Figure 2, thin sheets produce smaller droplets than jets, yet carry much larger flow rates due to the larger nozzle area.

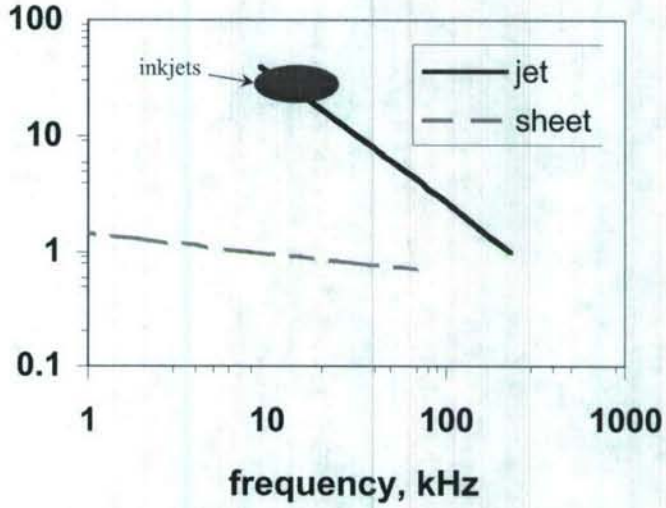

Figure 2. Dependence of droplet size on the forcing frequency

In general there are three modes of sheet disintegration; rim, perforated sheet and wave (shown in Figure 3). Viscous fluids tend to breakup via rim disintegration; the surface tension forces at the edge of the sheet contract it into a thick rim, which forms large droplets. A liquid sheet can be stretched to the point that small holes appear, enlarge and break the sheet into threads (perforated sheet disintegration). The threads then break up into small droplets. Lastly, wave motion disintegration of a thin sheet of fluid begins with instabilities that cause a portion of the sheet to tear away. Surface tension forces then contract and roll the sheet into ligaments, which fairly quickly disintegrate into micron-size droplets (Figure 3). We expect thin sheet disintegration to occur through either perforated sheet or wave motion disintegration or both. In any case, sheet disintegration tends to be less orderly than that for the laminar jet and will thus produce a greater distribution of droplet sizes.

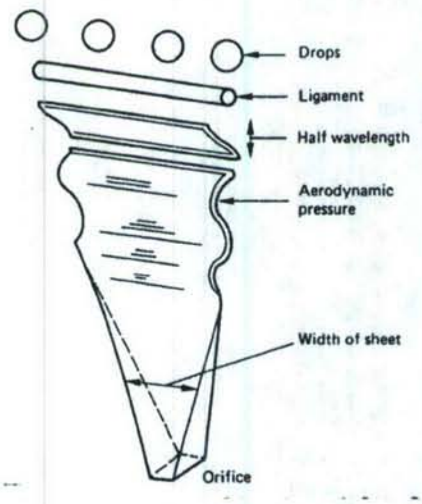

Figure 3. Sheet disintegration.

Just as the droplet size is proportional to the jet diameter for Rayleigh breakup, research has shown that the Sauter-mean diameter is proportional to $t^{0.4}$ for mm-thick sheets. While macro-scale derived correlations may not apply to μm-thick sheets, data at the micro-scale is not available. Thus, empirically derived expressions for droplet size were still used for analysis assuming $t_s = 2.0$ µm (2 μm x 650 μm nozzle), $C_D = 0.6$ and $u_{jet} = 1.0$ m/s (Re = 0.63). Since the correlation is a function of Weber number, the air cross-flow velocity was varied from 1.0 m/s to the subsonic velocities typical in a PDE inlet.

$$d_{3,2} = 0.071\left(\frac{t_s X \sigma \mu^{0.5}}{\rho^{0.5} u_{jet}^2}\right)^{1/3} \quad with \quad X = 0.123 t_s^{0.5} We^{-0.5}\,\mathrm{Re}^{0.6}$$

$$\text{and } f = \frac{u_{jet}}{\lambda_{opt}} \quad with \quad \lambda_{opt} = \frac{4\pi\sigma}{\rho_{air} u_{air}^2}$$

Very small droplets appear feasible and the required forcing frequency to resonate a liquid sheet is considerably less than that for a laminar jet in order to obtain the same droplet size (refer to Figure 2). The expelled volume of a liquid sheet is orders of magnitude greater than that of a laminar jet, showing great potential for this approach to attain high flow rates. It would take hundreds of small diameter nozzles to achieve the same volumetric flow.

b) Mass Flow Rate

The achievable mass flow rate of a large array atomizer will be largely a function of the droplet diameter, operating frequency, the mass per ejection pulse (influenced by the pressure/time relation of the forcing method), and nozzle array size. An upper design limit of 10 microns SMD at a mass flow rate of 0.5 lbm/sec (227 gm/sec) was imposed by the Navy as part of our Phase I study. The maximum operating frequency currently achieved by commercial inkjet technology is about 100 kHz. If each injector element were to eject one 10 μm droplet each pulse, at 100 kHz about five-million elements would be required to deliver 0.5 lbm/sec. At 600 dpi, this would require a surface area of about 13 in^2, not entirely unreasonable. However, the high frequency, power requirements and fabrication challenges make incorporating this many elements a formidable undertaking.

As observed above, however, sheet injection not only offers the potential of smaller droplets for the same minor dimension and Reynolds number, but can deliver much larger overall flow if large aspect ratios are used. Indeed, for a given droplet size, one can use a larger minor dimension with a slot jet than with a round hole, resulting in an even larger mass flow rate advantage. To illustrate the advantage of slot injection consider the following example. A 50 µm by 1 cm slot delivering at 1 m/sec results in a flow rate of 4 x 10^{-4} kg/sec. To deliver 5 lbm/sec would require only about 568 elements. If the thickness of each element is 1 mm, then the total injector footprint would be about 8.8 in^2.

c) Resulting Design Concepts

With the above discussion in mind, we generated a number of preliminary design concepts. The design drivers included power consumption, temperature sensitivity, mass injected per pulse and mass flux. Because of the first two drivers, we have chosen to utilize electrostatic actuation, rather than thermal or piezoelectric actuation. Thermal actuation is power intensive while piezoelectric materials are strongly temperature dependent and are more complex to fabricate.

The mass that a given diaphragm can displace is proportional to its surface area and average displacement. Figure 4 shows the number of 10 μm diameter droplets than can displaced by a circular diaphragm as a function of diaphragm radius (taking structural issues and reasonable voltage levels into account.) As can be seen, for quite reasonable diaphragm sizes, mass equivalent to large numbers of droplets can be ejected. For this reason, it is desirable to utilize larger diameter diaphragms. If the diaphragm is large enough, then it can be used to drive flow through multiple nozzles. Note that the diaphragm does not need to be round, although round diaphragms experience lower edge stress than rectangular configurations.

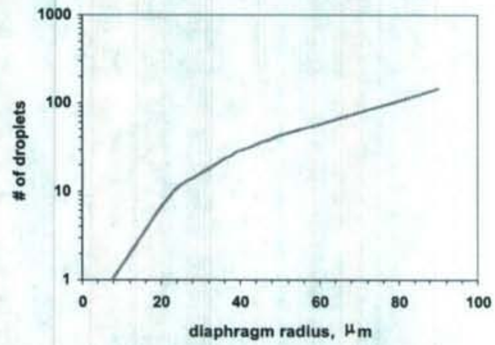

Figure 4 - Diaphragm sizing based on droplet production and structural limitations

After a number of design iterations we have converged on designs based on using slot injection and electrostatically activated double action diaphragm pumps using passive valving to generate net flow. This is shown conceptually in Figure 5.

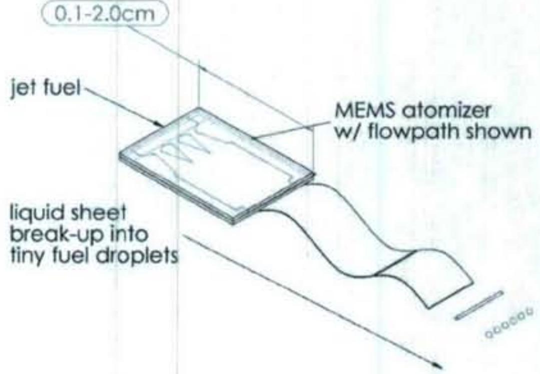

Figure 5. Conceptual drawing of a diaphragm pump activated slot injector.

Under ONR support we fabricated pump components for a range of pump sizes. Figure 6a shows a design with a rectangular diaphragm and Figure 6b a design with a round diaphragm. Both of these designs utilize converging/diverging nozzles as passive valves. We discuss the effectiveness of these and other passive valve configurations below.

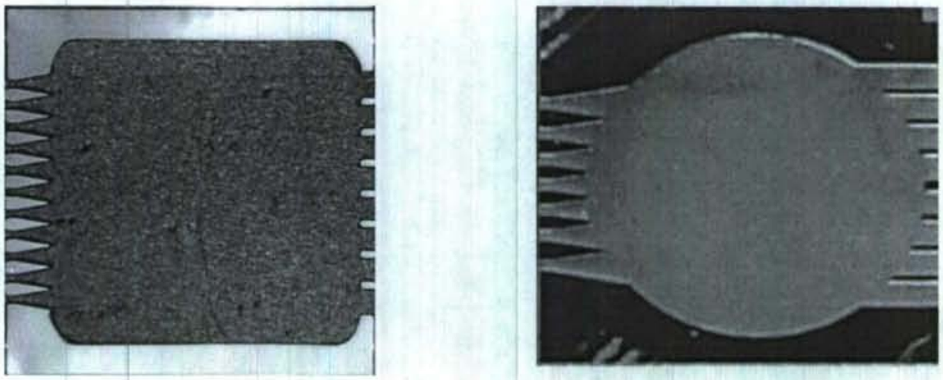

Figure 6. a) Square Diaphragm Design; b) Round Diaphragm Design

Both configurations were fabricated and assembled into prototypes by TDA Research, which were then tested at CU under the ONR Phase II SBIR. The experimental results were reported in Reference 5. Figure 10a shows a packaged device with electrical connections and flow fitting. Figure 7b is a view of the polished slot exit of the injector.

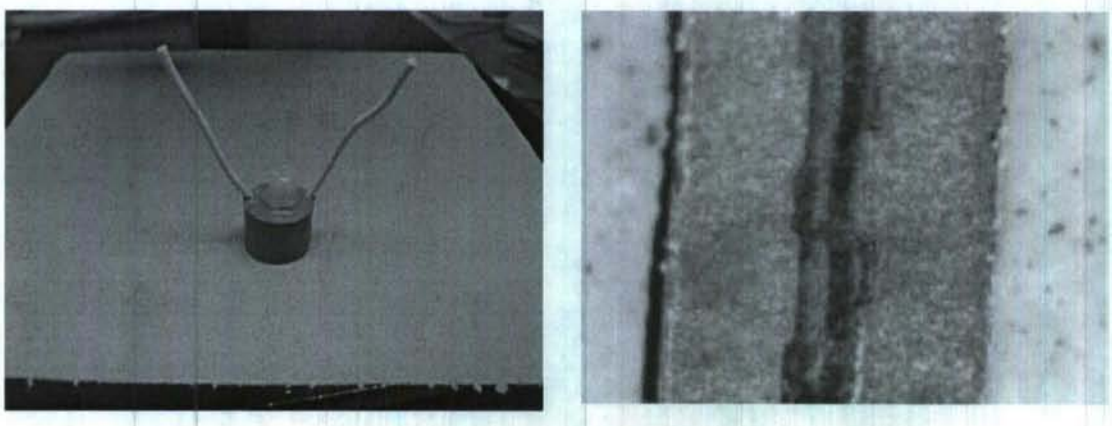

Figure 7. a) Packaged injector. b) View of slot exit following polishing.

d) Fluidic Diode Analysis

As with all diaphragm pumps, some means of preventing back flow is required. Early on we explored using mechanical check valves. However, the fabrication and packaging challenges are formidable. (In fact, we have fabricated a number of different valve designs, but decided the level of complexity involved was too great at this time in the development process.) In order to regulate the direction of flow, we have chosen to work with fluidic diodes, often called passive valves in the literature.

To analyze the effectiveness of various design concepts, flow was modeled using ANSYS, the commercial multi-physics finite element code. Forward and reverse flow velocity vectors are shown in Figures 7-10 (left-hand and right-hand columns, respectively) for a simple converging/diverging design and several Tesla configurations. The fluidic diode approach results in a highly reliable and passive valve that has little pressure drop for the forward flow. Biased flow resistance with respect to the backward flow occurs due to the asymmetric geometry. The increased flow resistance can be caused by separated flow, flow reversal or interference.

In the case of the diffuser the forward flow enters the nozzle via a rounded inlet and is then gradually diffused to low velocity without flow separation for delivery to the atomizing chamber. Resistance to flow in the diffuser direction is less than that in the back flow direction. Figure 11 shows the calculated steady-state discharge coefficient ratio for the nozzle/diffuser configuration. Forward flow passes smoothly through a Tesla diode, but in the reverse direction a large percentage of the flow is now bypassed to create an impinging jet that obstructs flow through the exit passage. There are many possible implementations of this strategy as shown in Figures 7-10.

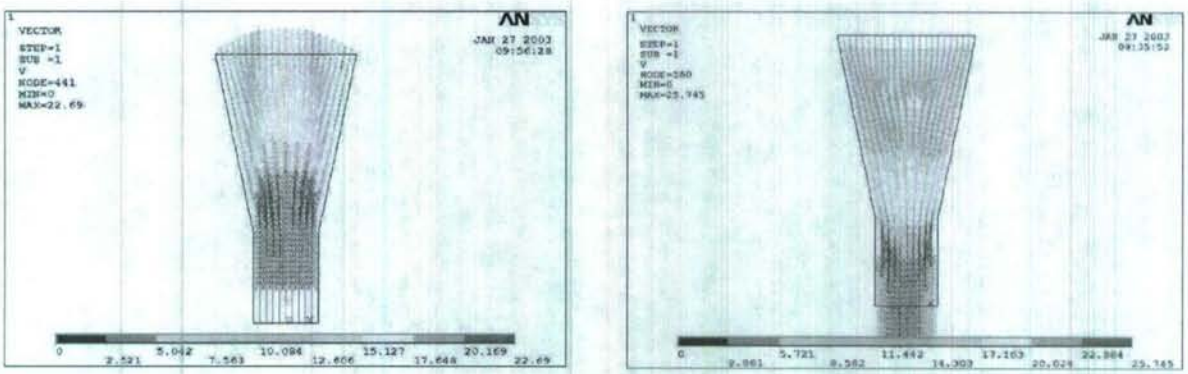

Figure 7. Nozzle/Diffuser Configuration

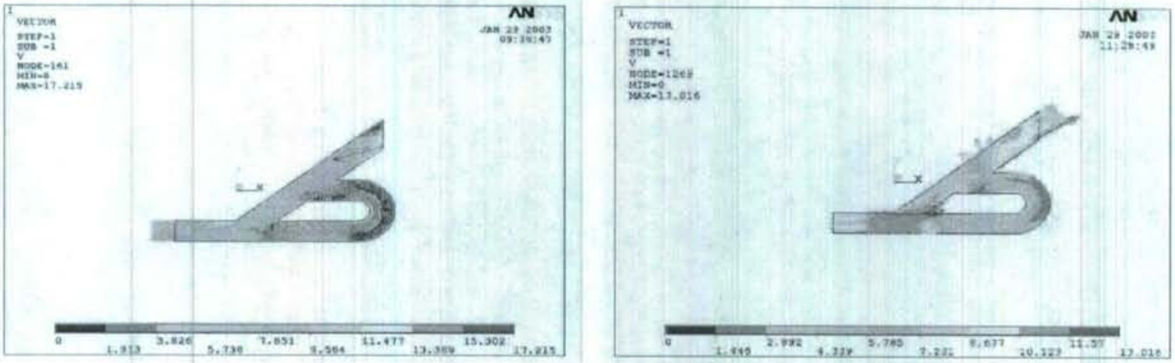

Figure 8. Tesla Diode #1

Figure 9. Tesla Diode #2

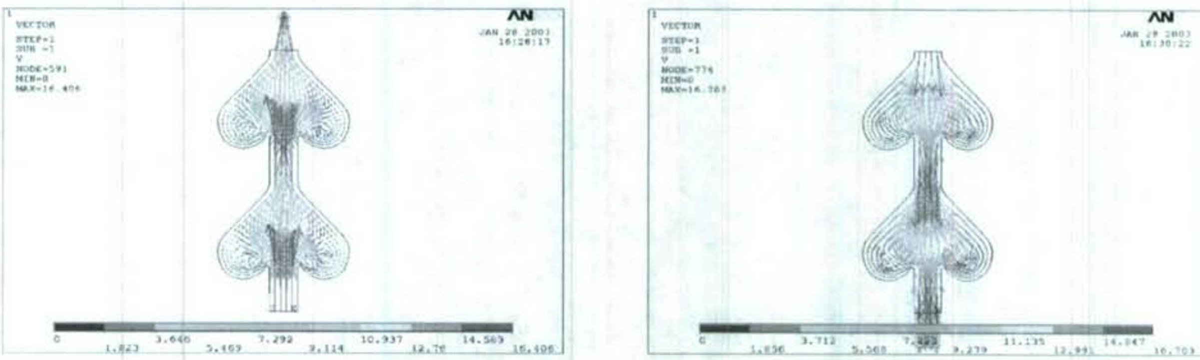

Figure 10. Sudden Expansion Tesla

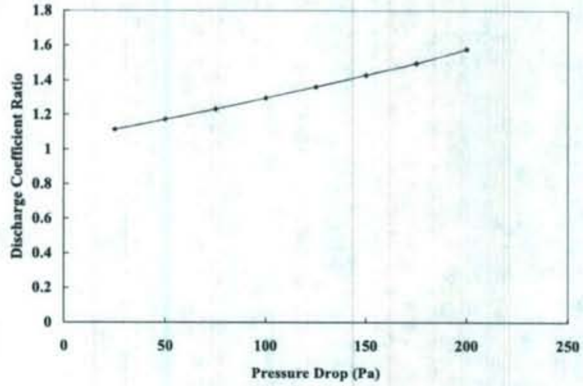

Figure 11. Discharge Coefficient Ratio for Nozzle/Diffuser Configuration

One interesting aspect of these small-scale valves is that, in practice, inertial effects can be quite important. We have carried out simple analytical modeling and showed that fairly large phase delays can result from inertia. Therefore, effective discharge ratios can be quite different than the steady-state values.

e) Whole Pump Simulations

Our first whole pump simulations were for a relatively simple design as shown in Figure 12. The square diaphragm is manufactured from nickel and has dimensions of 1mm x 1mm x 50 μm. The depth of the chamber below the diaphragm is 100 μm. The inlet and outlet channels are also 100 μm deep and in the same plane as the plenum under the diaphragm. They are each 0.33 mm long and have an entry that is 66.7 mm wide. They expand with a half angle of five degrees, so the exit width is 124.5 μm. Typically, each end is attached to a manifold of large cross sectional area.

Calculations were carried out for frequencies ranging from 100-900 Hz. Figure 13 shows the diaphragm displacement for 500 Hz. As can be seen the displacement is almost purely sinusoidal with no obvious startup transient. This is the case for all the frequencies simulated. Figure 14 shows the pressure following startup. In this case, a clear starting transient is observed that is still dying out as the simulation proceeds. Figure 15 shows the instantaneous volume flow rates as a function of time through a single pump cycle (at 700 Hz in this case.) Plotted are the flow rate out of the inlet, out of the outlet and the net flow rate. The integral of the net flow over a complete cycle, which equals the average flow rate, is plotted in Figure 16 as a function of the frequency. The natural frequency of the diaphragm alone is about 103,000 Hz. Adding the fluid mass lowers it to about 93,520 Hz. At the voltages required, it is difficult to provide switching electronics that can operate very far above about 1000 Hz. Therefore, in this example we are operating far below the resonant frequency. The numerical and analytic results are in good agreement.

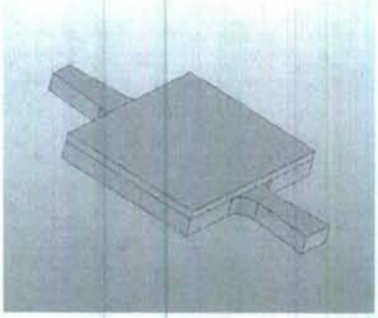

Figure 12. Solid drawing of the pump

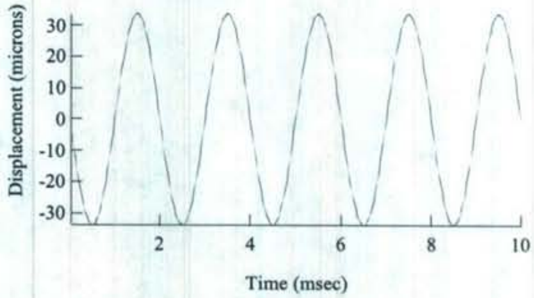

Figure 13. Diaphragm displacement at 500 Hz

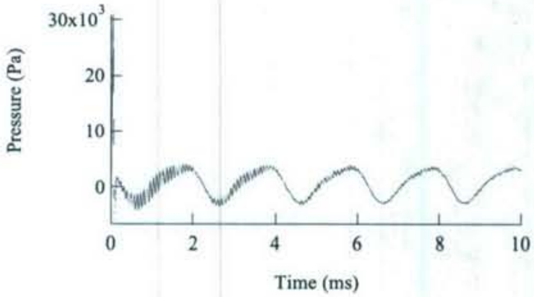

Figure 14. Pressure at 500 Hz

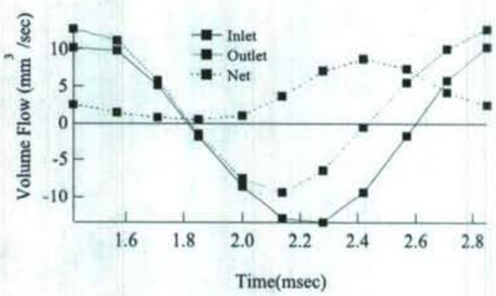

Figure 15. Flow Rates at 700 Hz

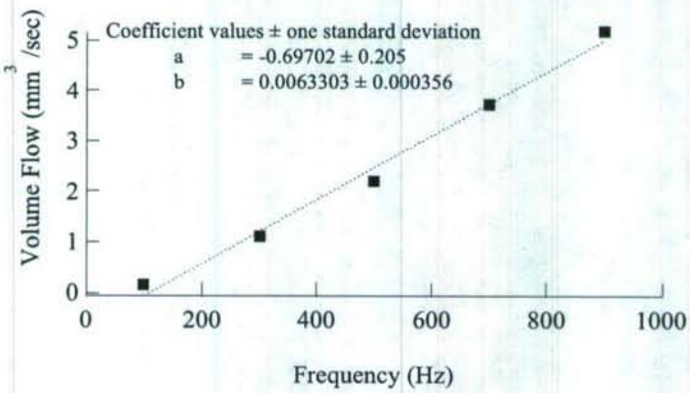

Figure 16. Net Volume Flow Rate through Pump

As discussed above, mass flow considerations lead to designs with fairly large diaphragms and we subsequently modeled such devices. Figure 17 shows axial velocity contours during the expulsion phase of the pump cycle for a 1 cm x 1 cm design using passive valves at the inlet and with a slot exit.

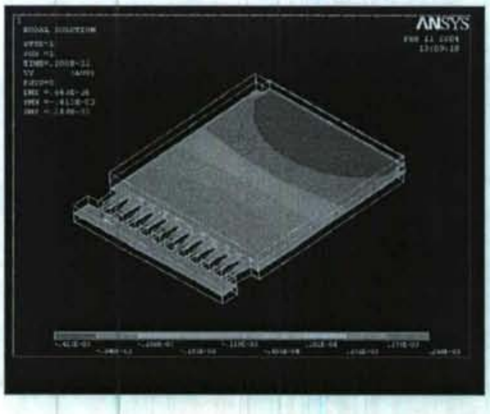

Figure 17. Contour Plot of Axial Velocity during expulsion phase of a 1 cm x 1 cm diaphragm pump.

f) Summary

Our findings showed that inkjet technology does have the potential to meet PDE fuel injection needs. Military fuel properties are suitable for micro injection. Mass flow demands can be met with large array injectors, areas on the order of 10 in^2 will be required to deliver 0.5 lbm/sec. By proper sizing and shaping of the injection slots, drop size requirements can be met.

Under AFOSR support we developed analytical and numerical tools to model MEMS scale atomizers. The analytical tools are useful for rough design assessments. Using the the multiphysics capabilities of ANSYS, we developed a complete numerical model of an atomizer. The numerical model was used to simulate designs in support of fabrication activities carried out under the ONR SBIR.

Under ONR support we fabricated the components for several competing designs, including active and passive valve designs and pump designs ranging from 200 μm to 1 cm in diaphragm dimension. We used MUMPS, SOIMUMPS, and conventional Very Large Scale Integrated Circuit (VLSIC) fabrication methods. We packaged and tested 1 cm pumps.

References

1. Nabity, J., G. Balducci and J.W. Daily, "Electrostatically Actuated Fuel Atomizer Design for the Pulse Detonation Engine," 39th AIAA/ASME/SAE/ASEE Joint Propulsion Conference and Exhibit, Paper Number 2003-4821, 2003.

2. Krishnan, G., J. W. Daily and J. Nabity, "Simulation of an Electrostatically Driven Microinjector," 42nd AIAA Aerospace Sciences Meeting and Exhibit, Paper Number 2004-0305, 2004.

3. James Nabity and John Daily, "A MEMS Fuel Atomizer for Advanced Engines," AIAA 2004-6711, presented at the CANEUS 2004: Conference on Micro-Nano-Technologies, Monterey, CA.1-5 November, 2004.

4. Krishnan, G., J.W. Daily, "Simulation of Large Membrane Deflection in a Micro Pump," VII International Conference on Microsystems, El Paso, TX 22 September, 2005.

5. Nabity, James, Sean Rooney, John Daily, Eric Johnson and Jean Hertzberg, "An Electrostatically Actuated MEMS Fuel Injector to Enhance Low-Pressure Atomization ," AIAA Aerospace Sciences Meeting, Paper AIAA 2006-804, 9-12 January, 2006.

6. Krishnan, G., J. W. Daily and J. Nabity, "Simulation of an Electrostatically Driven Microinjector," To appear in the AIAA Journal of Propulsion and Power, 2007.

7. J. Nabity, G. Balducci and J. Daily, Liquid Fuel Atomizer Phase I Final Report, ONR SBIR Contract N00014-01-M-0036, June, 2001.

8. J. Nabity, TDA Research and G. Krishnan and J. Daily, University of Colorado at Boulder, _Phase II Interim Report (Oct 15, 2003 _ Jan 14, 2004): Liquid Fuel Atomizer,_ ONR SBIR Contract N00014-01-C-0457, Feb, 2004.

9. James Nabity, "Liquid Fuel Atomizer," SBIR Phase II Final Report for ONR contract #N00014-01-C-0457, TDA Research, Inc., 2005.